ChemComm

Dynamic Article Links

Cite this: *Chem. Commun.*, 2012, **48**, 9159–9161

www.rsc.org/chemcomm

COMMUNICATION

Electrocatalytic reduction of coreactant by highly loaded dendrimer-encapsulated palladium nanoparticles for sensitive electrochemiluminescent immunoassay†

Shengyuan Deng, Jianping Lei, Yin Huang, Xiaonan Yao, Lin Ding and Huangxian Ju*

Received 13th June 2012, Accepted 25th July 2012
DOI: 10.1039/c2cc34221a

Dendrimer-encapsulated palladium nanoparticles anchored on a carbon nanohorn were designed as a nonenzymatic tracing tag for sensitive quantum dot-based electrochemiluminescent immunoassay by electrocatalytic reduction of dissolved O_2 as the coreactant.

The quantum dots (QDs)-based electrochemiluminescent (ECL) immunoassay has been rapidly developed owing to its intrinsic low background and high sensitivity.[1] The two main methodologies include: steric hindrance resulting from the formation of an immunocomplex and consumption of ECL coreactant in an enzymatic reaction.[2] To accurately determine biomarkers at ultralow levels, signal amplification strategies based on enzyme loaded carriers as tracing tags have been proposed to enhance signal transduction of recognition events.[3] For example, gold nanoparticles have been used as DNAzyme carriers for ultrasensitive ECL immunoassays.[4] However, these strategies usually suffer from specific catalytic substrates, costly engineering and purification processes of enzymes, and easy loss of bioactivity.[5] Hence, an alternative nonenzymatic tag is urgently needed.

Compared with the enzyme-linked tags, nanomaterials have shown great promise as nonenzymatic tags due to the capability of high electrocatalytic reactivity toward O_2 reduction.[6] A signal-on sandwich immunoassay based on the ECL of QDs has been proposed by an adsorption-induced catalytic reduction of dissolved O_2 at the sidewall of N-doped carbon nanotubes.[7] Nanohybrid-based tracing tags can not only amplify the recognition events by enzymatic mimicking activity,[8] but can improve the conductivity and biocompatibility of biosensing interfaces to accelerate the signal transduction. In this work, a further novel tracing tag was designed with highly efficient electrocatalytic ability toward the reduction of ECL coreactant by functionalizing a single-walled carbon nanohorn (SWNH) with dendrimer-encapsulated palladium nanoparticles (PdNPs).

State Key Laboratory of Analytical Chemistry for Life Science, School of Chemistry and Chemical Engineering, Nanjing University, Nanjing 210093, P.R. China. E-mail: hxju@nju.edu.cn

† Electronic supplementary information (ESI) available: Experimental details, spectroscopic and morphology characterization, optimal conditions and sensing performance. See DOI: 10.1039/c2cc34221a

SWNHs are composed of thousands of graphitic tubules terminated with highly defective cone-shaped horns and have a large surface area. The oxidation treatment of a SWNH can produce extensive oxygenate sites exposed on the tips as a scaffold for immobilization of biomolecules.[9] This work firstly used dendrimers to functionalize the SWNH for further improvement of biocompatibility, while utilizing the numerous internal groups of the dendrimers to adsorb $PdCl_4^{2-}$. Upon a chemical reduction process, PdNPs with a narrow size distribution can be formed in the interior structure of a dendrimer. Thus a nanocatalyst, highly loaded dendrimer-encapsulated PdNPs anchored on a SWNH (PdNPs@PMM5/SWNH), was obtained using amine-terminated generation 5.0 polyamidoamine (PMM5) for electrocatalytic reduction of O_2 as an efficient coreactant-scavenger candidate for QD-based ECL emission (Scheme 1). Combining the novel functional nonenzymatic tag with the low-potential ECL emission of around 620 nm of bidentate-chelated CdTe QDs led to a sensitive 'signal-off' ECL immunosensor.[10] Using carcinoembryonic antigen (CEA) as a model, this immunoassay method showed a wide linear range and a detection limit down to the sub-picomolar level, facilitating the screening of CEA at the early stage of cancers. The proposed nanohybrid as a tracing tag introduces a new concept of signal amplification for detection of cancer biomarkers in ultrasensitive bioanalysis.

The SWNHs showed round-shaped aggregates of 100 nm in diameter associated with typical tubes (Fig. S1A in ESI†),

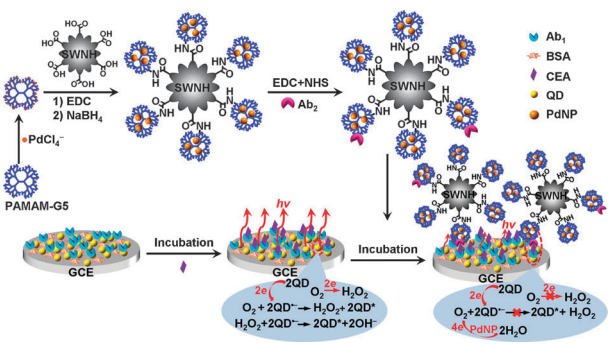

Scheme 1 Schematic representation of preparations of tracing tag, and ECL annihilation strategy by electrocatalytic reduction towards dissolved O_2 at PdNPs@PMM5/SWNH nanohybrids.

leading to an extra-large surface-to-volume ratio. The stress–strain effect over the cones made SWNHs susceptible to oxidation producing abundant O-functionalities. After an amide was introduced between the primary amines of PMM5 and the carboxylated SWNHs, the transmission electron microscopic (TEM) image of PMM5/SWNHs showed a similar resemblance (Fig. S1B in ESI†), indicating the functional process preserved the original structure of the SWNH. The electrostatic repulsions among the protonated amines at low pH produced extended starburst conformations of dendrimers, which facilitated the penetration and anchoring of $PdCl_4^{2-}$ onto amines. After subsequent reduction, the formed PdNPs@PMM5/SWNHs showed well-distributed and size-uniform particles with a mean size of about 3 nm (Fig. S1C and D in ESI†).[11] The high-resolution TEM (HRTEM) image clearly showed roughly spherical PdNPs suspended within the branched PMM5 (Fig. S1E in ESI†), which was quite different from the direct growth of PdNPs on SWNHs or straight-chain polymers with few particles and a broad size distribution.[12] The SEM images displayed a morphology change after associating PdNPs@PMM5/SWNHs with the signal antibody (Ab_2). PdNPs@PMM5/SWNHs appeared as grain-like particles (Fig. S1F in ESI†), while Ab_2/PdNPs@PMM5/SWNHs became viscous (Fig. S1G in ESI†),[13] indicating that Ab_2 were successfully loaded due to the specific recognition of the tracing tag to target antigen.[3a,14] The obtained tracing tag could be well dispersed in physiological buffer (Fig. S1H in ESI†), thus was favorable for bioassay.

The formation of PdNPs@PMM/SWNHs and Ab_2 labeling to the nanohybrids were further confirmed with FT-IR spectra and X-ray photoelectron spectroscopy (Fig. S2 in ESI†), while atomic force microscopic images (Fig. S3 in ESI†) and electrochemical impedance spectra (Fig. S4A in ESI†) were utilized to monitor the sequential fabrication of the immunosensor and the recognition of carcinoembryonic antigen. The bare glassy carbon electrode (GCE) showed a relatively small charge-transfer resistance (R_{ct}), while the R_{ct} of the QDs modified GCE became 914 Ω due to the intrinsic semiconductivity (Fig. S4A, curves a and b in ESI†). An increase in R_{ct} was observed during the stepwise attachment of primary antibody (Ab_1), bovine serum albumin (BSA), antigen and the tracing tag due to their insulating properties (Fig. S4A, curves c to f in ESI†), verifying their immobilization.

A comparison of ECL signals in the preparation of the immunosensor and in the sandwich detection of CEA is shown in Fig. S4B (ESI†). The QDs film showed a strong ECL emission in air-saturated PBS with a relatively low peak potential at −0.93 V. After chitosan and Ab_1 were assembled, a decrease in intensity by 15% was observed. The further drop in intensity was produced by blocking non-specific binding sites with BSA. Meanwhile, the peak potential negatively shifted from −0.96 V to −1.0 V due to the barrier of inert proteins to electrons and mass transfer of dissolved O_2 as coreactant. The subsequent incubation in 100 ng mL^{-1} CEA and mere Ab_2 rendered additional 5% and 8% decreases in ECL intensity, respectively. However, when Ab_2/PdNPs@PMM5/SWNH was applied, the ECL intensity decreased by 62%. The much larger quenching percentage should be ascribed

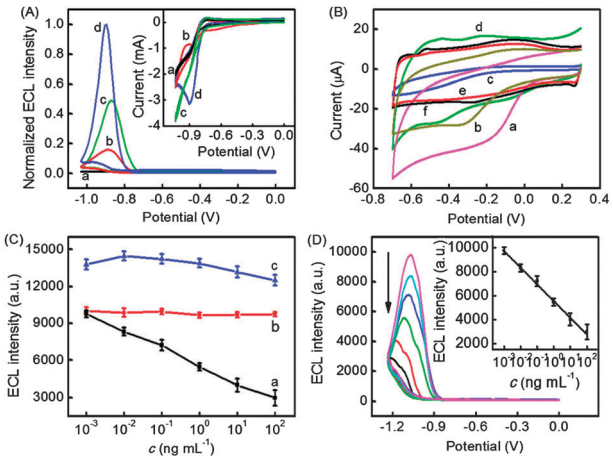

Fig. 1 (A) ECL-potential curves of QDs modified GCE in N_2-saturated (a), air-saturated (b), 320 μM H_2O_2 + N_2-saturated (c) and O_2-saturated (d) pH 9.0 PBS. Inset: corresponding CVs. (B) CVs of PdNPs@PMM5/SWNHs (a), PdNPs@PMM4/SWNHs (b), PdNPs@PMM5 (c), PdNPs/SWNHs (d), PMM5/SWNHs (e) and SWNHs (f) modified GCE in air-saturated pH 9.0 PBS. (C) ECL responses of immunosensor to CEA concentration in the presence (a) and absence (b) of Ab_2-tag in air-saturated pH 9.0 PBS, and in the presence of Ab_2-tag in N_2-saturated pH 9.0 PBS containing 1 mM $K_2S_2O_8$ (c). (D) ECL response of immunosensor to 0.001, 0.01, 0.1, 1, 10 and 100 ng mL^{-1} CEA (from top to bottom). Inset: calibration curve.

to the electrocatalytic reduction of dissolved O_2 by PdNPs, which consumed O_2 and decreased the concentration of coreactant for generating ECL emission on the electrode surface.

The QDs modified GCE could be reduced in O_2-free pH 9.0 PBS with a cathodic wave peaking at −0.90 V (Fig. 1A, curve a in inset) without ECL emission (Fig. 1A, curve a). In air-saturated PBS, the cyclic voltammogram (CV) showed a weak reduction peak at –0.64 and a relatively strong reduction peak at −0.90 V (Fig. 1A, curve b in inset), which was attributed to the reduction of O_2 and QDs, respectively,[10] while a low-potential ECL emission peaking at −0.90 V was observed (Fig. 1A, curve b). The ECL signals could keep stable for around 10 cycles up to 240 s after the first cycle. The ECL emission in O_2-free PBS contained 320 μM H_2O_2, whose concentration approximated the saturated concentration of dissolved O_2 under the standard atmospheric pressure at room temperature, suggesting H_2O_2 was a coreactant (Fig. 1A, curve c). However, in O_2-saturated pH 9.0 PBS (Fig. 1A, curve d) the ECL emission showed an intensity about twice that observed in curve c. As a consequence, O_2 was a more efficient coreactant than H_2O_2 for ECL of QDs since it could capture more electrons from electro-reduced QDs than H_2O_2 and their reaction rates were also different.[15] The negative shift of ECL peak potential in O_2-saturated PBS by 20 mV was due to the high O_2 concentration according to the Nernst equation. Although the O_2 concentration was higher in O_2-saturated PBS than in air-saturated PBS, its reduction wave did not increase observably (Fig. 1A, curves b and d in inset), whereas the ECL intensity became much greater (Fig. 1A, curves b and d), indicating that O_2 was the main and direct coreactant (Formula (1)–(5) in ESI†).

In air-saturated pH 9.0 PBS, the PdNPs@PMM5/SWNHs and PdNPs@PMM4/SWNHs modified electrodes showed a cathodic peak at −0.15 and −0.3 V with peak currents of 39.1 and 24.4 μA (Fig. 1B, curves a and b), respectively, indicating obvious electrocatalytic activity of PdNPs@PMM/SWNHs toward O_2 reduction and indicating that PMM5 carried more PdNPs than PMM4 for electrocatalysis. PdNPs@PMM5 and PdNPs/SWNHs modified electrodes showed a peak current of only 11.8 μA and much weaker responses (Fig. 1B, curves c and d). Obviously SWNHs promoted the electron transfer and the direct growth of PdNPs on SWNHs produced low loading of PdNPs. The SWNHs and PMM5/SWNHs modified electrodes showed a couple of small peaks at around −0.28 V (Fig. 1B, curves e and f), which were derived from the reduction of some O-functional groups on SWNHs. Since O_2 acted as the coreactant of QD-based ECL, the presence of PdNPs@PMM5/SWNHs could antagonistically consume the coreactant *via* electrocatalytic reduction and prohibit the formation of the excited state (QD*), quenching the ECL emission. Thus PdNPs@PMM5/SWNHs could be used as a novel tracing tag for a QD-based ECL immunoassay (Scheme 1).

The ECL immunosensing methods developed mainly include two mechanisms: steric hindrance produced from the formation of an immunocomplex, and consumption of ECL coreactant. As shown in Fig. 1C, the ECL intensity decreased with increasing CEA concentration (curve a), which was attributed to the consumption of dissolved O_2 through its electro-reduction catalyzed by PdNPs@PMM5/SWNHs. Relatively, the contribution of steric hindrance to ECL quenching even at high CEA concentrations (*e.g.* 100 ng mL^{-1}) was much lower (curve b). Furthermore, replacing O_2 with $K_2S_2O_8$ also did not show a sensitive linearity (curve c), validating that the proposed coreactant consumption strategy was more sensitive than the steric hindrance one. Thus, the electro-reduction of dissolved O_2 due to the presence of the tracing tag as a mimicking enzyme played a key role in the ECL immunosensing.

Under the optimum conditions (Fig. S5 in ESI†), the ECL intensity of the immunosensor decreased with increasing concentration of CEA along with a shift in the peak potential from −1.05 to −1.16 V (Fig. 1D). The calibration plot showed a good linear relationship between the ECL peak intensity and the logarithm value of CEA concentration ranging from 100 ng mL^{-1} to 1 pg mL^{-1} with a correlation coefficient of 0.996 (inset in Fig. 1D). The detection limit was 0.47 pg mL^{-1} (S/N = 3), which was lower than 1.4 pg mL^{-1} by electrochemical immunoassay using glucose oxidase functionalized carbon nanotubes as the trace label.[16] More importantly, this immunoassay showed a wide detection range of 6 orders of magnitude and avoided deoxygenation in the immunoassay.

The ECL immunosensor showed good stability and reproducibility (Fig. S6 in ESI†). The analytical reliability and application potential of the proposed method were evaluated by comparing assay results of clinical serum samples with reference values from commercial ECL single-analyte tests (Table S1 in ESI†). Considering the CEA threshold of 5 μg mL^{-1} for clinic diagnoses, the proposed method possessed good practicability.[17]

In conclusion, a dendrimer-encapsulated PdNPs anchored SWNH tag was successfully designed for sensitive immunoassay. The *in situ* reduction of $PdCl_4^{2-}$ adsorbed inside SWNH-supported PMM greatly improved the loading capacity of PdNPs and the aqueous dispersion of the nanohybrids for labeling. The nanohybrids, as enzyme mimicks, could efficiently electro-catalyze the reduction of dissolved O_2. Based on the consumption of O_2 as endogenous coreactant, a facile ECL platform was proposed. The ECL immunoassay method showed a wide detection range with low detection limit and acceptable precision. To the best of our knowledge, this is the first time metallic nanoparticles have been used as the mimicking enzyme for QD-based ECL. This novel functional tracing tag could achieve promising applications in determination of low-abundant biomarkers.

This work was financially supported by the National Basic Research Program of China (2010CB732400), National Natural Science Foundation of China (21121091, 21135002).

Notes and references

1 R. Gill, M. Zayats and I. Willner, *Angew. Chem., Int. Ed.*, 2008, **47**, 7602–7625.
2 J. P. Lei and H. X. Ju, *TrAC, Trends Anal. Chem.*, 2011, **30**, 1351–1359.
3 (*a*) J. Das, H. Kim, K. Jo, K. H. Park, S. Jon, K. Lee and H. Yang, *Chem. Commun.*, 2009, 6394–6396; (*b*) V. Mani, B. V. Chikkaveeraiah, V. Patel, J. S. Gutkind and J. F. Rusling, *ACS Nano*, 2009, **3**, 585–594.
4 D. J. Lin, J. Wu, F. Yan, S. Y. Deng and H. X. Ju, *Anal. Chem.*, 2011, **83**, 5214–5221.
5 B. S. Munge, A. L. Coffey, J. M. Doucette, B. K. Somba, R. Malhotra, V. Patel, J. S. Gutkind and J. F. Rusling, *Angew. Chem., Int. Ed.*, 2011, **50**, 7915–7918.
6 (*a*) R. Polsky, J. C. Harper, D. R. Wheeler, S. M. Dirk, J. A. Rawlings and S. M. Brozik, *Chem. Commun.*, 2007, 2741–2743; (*b*) H. B. Yildiz, R. Freeman, R. Gill and I. Willner, *Anal. Chem.*, 2008, **80**, 2811–2816.
7 S. Y. Deng, Z. T. Hou, J. P. Lei, D. J. Lin, Z. Hu, F. Yan and H. X. Ju, *Chem. Commun.*, 2011, **47**, 12107–12109.
8 L. Z. Gao, J. Zhuang, L. Nie, J. B. Zhang, Y. Zhang, N. Gu, T. H. Wang, J. Feng, D. L. Yang, S. Perrett and X. Y. Yan, *Nat. Nanotechnol.*, 2007, **2**, 577–583.
9 (*a*) M. Zhang, M. Yudasaka, K. Ajima, J. Miyawaki and S. Iijima, *ACS Nano*, 2007, **1**, 265–272; (*b*) M. Zhang, T. Murakami, K. Ajima, K. Tsuchida, A. S. D. Sandanayaka, O. Ito, S. Iijima and M. Yudasaka, *Proc. Natl. Acad. Sci. U. S. A.*, 2008, **105**, 14773–14778.
10 X. Liu, L. X. Cheng, J. P. Lei, H. Liu and H. X. Ju, *Chem.–Eur. J.*, 2010, **16**, 10764–10770.
11 A. M. Caminade and J. P. Majoral, *Chem. Soc. Rev.*, 2010, **39**, 2034–2047.
12 E. Bekyarova, A. Hashimoto, M. Yudasaka, Y. Hattori, K. Murata, H. Kanoh, D. Kasuya, S. Iijima and K. Kaneko, *J. Phys. Chem. B*, 2005, **109**, 3711–3714.
13 J. Zhang, J. P. Lei, C. L. Xu, L. Ding and H. X. Ju, *Anal. Chem.*, 2010, **82**, 1117–1122.
14 J. S. Jirkovsk, I. Panas, E. Ahlberg, M. Halasa, S. Romani and D. J. Schiffrin, *J. Am. Chem. Soc.*, 2011, **133**, 19432–19441.
15 H. Jiang and H. X. Ju, *Chem. Commun.*, 2007, 404–406.
16 G. S. Lai, F. Yan and H. X. Ju, *Anal. Chem.*, 2009, **81**, 9730–9736.
17 S. Ishigami, S. Natsugoe, S. Hokita, X. M. Che, K. Tokuda, A. Nakajo and H. Iwashige, *J. Clin. Gastroenterol.*, 2001, **1**, 41–44.